

# Analyzing Pantheon SNeIa data in the context of Barrow's variable speed of light

Hoang Ky Nguyen\*

Department of Physics, Babeş-Bolyai University, Cluj-Napoca 400084, Romania

(Dated: April 4, 2024)

We analyze the Combined Pantheon Sample of Type Ia supernovae while allowing the velocity of light to vary as a function of the scale factor  $c \propto a^{-\zeta}$ , as initiated by Barrow [Phys. Rev. D **59**, 043515 (1999)]. The variation in the velocity of light creates an effect akin to the refraction phenomenon which occurs for a wave traveling in a medium with varying speed of wave. We elucidate the role of the local scale of gravitationally-bound regions *in assisting the refraction effect to manifest*. The refraction effect alters the redshift formulae (Lemaître, distance-vs- $z$ , luminosity distance-vs- $z$ ) and warrants a new analysis of the Pantheon dataset. Upon a reformulation of the distance-redshift relations, we achieve a high-quality fit of the Pantheon dataset to the variable light speed approach; the fit is as robust as that obtained in the standard  $\Lambda$ CDM model. We find that the Pantheon dataset is consistent with the variable light speed of the functional form:  $a \propto t^\mu$  and  $c \propto a^{1-1/\mu}$  with (i) the cosmic age  $t_0 \approx 13.9$  Gy as a free parameter, while  $\mu$  is unspecified; and (ii) a monotonic variation in the local scale for gravitationally-bound objects (applicable to the emission sources and the Solar System-based apparatus/observer). Due to the agent in (ii), the high- $z$  portion of the Pantheon dataset would produce an “effective”  $H_0$  estimate which is 10 percent lower than the  $H_0$  estimate obtained from the low- $z$  portion of the dataset. We offer an alternative interpretation of the accelerating expansion by way of variable speed of light, and as a by-product of the agent uncovered in (ii), a tentative suggestion toward “resolving” the ongoing tension in the Hubble constant estimates.

## I. MOTIVATION

The possibility of variation in the velocity of light was first advocated by Einstein in 1911 [2] in his search for a formulation of General Relativity (GR). As he emphasized in [3, 4], his consideration of variable velocity of light is not in contradiction with the principle of the constancy of the velocity of light. This is because the latter, or equivalently the Michelson-Morley experimental result and the Lorentz invariance, is meant to be valid only *locally*. At a given point on the manifold, the set of tangent frames satisfy the Lorentz invariance with a common value of  $c$ . However, Einstein recognized that the value of  $c$  in principle may vary on the manifold. In the language of the geometry, whereas the speed of light is an *invariant* (meaning that  $c$  is unaffected upon a general coordinate transformation), it can be *position-dependent*, viz.  $c(x^\mu)$ . The speed of light in principle can be a scalar field, rather than a universal constant. In Ref. [2], Einstein explicitly allowed the gravitational field to influence the value of  $c$ .<sup>1</sup>

The modern form of variable speed of light (VSL hereafter) was revived in the work of Moffat in 1992 [5] and independently by Albrecht and Magueijo in 1998 [6] in the context of early-time cosmology. Their proposals aimed to resolve the horizon puzzle while avoiding the need for

cosmic inflation. Several scholars explored different aspects of the VSL, most notably being [1, 7–11].

The application of VSL in late-time cosmology, mostly to analyzing the Type Ia supernovae (SNeIa) data, has been more limited, apparently without clear successes [12–15]. Upon reviewing these works, we conclude that they continued to rely on the classic Lemaître redshift formula, viz.  $1 + z = a^{-1}$ . We believe that this is an oversight, however. There are certain types of VSL in which the classic Lemaître redshift formula is no longer applicable, warranting a revision. One such type of VSL exists in the form of the velocity of light being dependent on the scale factor, e.g.  $c \propto a^{-\zeta}$ , a form first employed by Barrow [1]. As will be shown in Section III C in this Report, as a traveling lightwave makes a transit between a gravitationally-bound region which resists cosmic expansion and an outer space region that is subject to cosmic expansion, *proper care is needed to handle the alteration of the wavelength*.<sup>2</sup> We find that transits of this type do introduce fundamental modifications to Lemaître's redshift formula. In particular, Barrow's VSL form  $c \propto a^{-\zeta}$  would result in a *modified* Lemaître formula:  $1 + z = a^{-(1+\zeta)}$ . We believe that the lack of progress in applying VSL to late-time cosmology has been due to the aforementioned oversight in missing out the VSL component (in Barrow's case, the exponent  $\zeta$ ) in the redshift relations. It is the purpose of our Report to

\* hoang.nguyen@ubbcluj.ro

<sup>1</sup> Note that the speed of light appears in two places: (1) in the underlying theory as an *invariant* and (2) in the metric which depends on the choice of ruler and clock. The speed of light that participates in the underlying theory is what Einstein intended and is the focus of our Report. We thank Viktor Toth for clarifying the distinct roles of  $c$  in the two places, (1) vs (2).

<sup>2</sup> Previous VSL works overlooked an additional alteration in the wavelength which takes place when the lightwave transits from the outer space region into the (gravitationally-bound) Milky Way to reach the Earth-based observer. See Section III C and Appendix A for our detailed rectification of the oversight.

properly sort out this intricacy.

In this Report, we apply Barrow's VSL form  $c \propto a^{-\zeta}$  into analyzing the SNeIa data and interpreting the accelerating expansion. As a lightwave travels from a distant emitter toward the Earth-based observer, if the velocity of light varies as a function the scale factor (with the latter meaning the global scale factor of the cosmos *and* the local scale factor of gravitationally-bound regions), the lightwave would undergo a refraction effect akin to the phenomenon which takes place as a physical wave travels in an inhomogeneous medium with varying speed of wave. That is how the exponent  $\zeta$  finds its way into the modified Lemaitre redshift formula,  $1 + z = a^{-(1+\zeta)}$ , alluded above. To our knowledge, this is the first time the refraction effect is explicitly considered for late-time cosmology.

The trove of data in the Combined Pantheon Sample [16, 17] enables our current study. The question we aim to address is whether the refraction effect induced by way of the VSL alone can account for the Pantheon dataset and provide a complete explanation of the accelerating expansion observed in SNeIa [18, 19]. This pursuit is legitimate: although GR has been verified in the scale of the solar system or that of binary stars, the Friedmann equations involve an extrapolation of GR onto the cosmic scales. This extrapolation constitutes a major assumption in cosmology [20]. As observational data of SNeIa did not fit with the original Friedmann framework, among other reasons, standard cosmology introduced new components such as the  $\Lambda$  term to account for the accelerating expansion. Our analysis presented in this Report does not resort to GR or the Friedmann equations. It is based on a quite generic and parsimonious setup without relying on an underlying theory of gravitation.

Our Report is structured as follows. In Section II we introduce a VSL modification in the Robertson-Walker metric. In Section III we derive the modified redshift relations (Lemaitre, distance-vs- $z$ , luminosity distance-vs- $z$ ) by enabling variation in the speed of light and variation in the local scale of the gravitationally-bound regions; *we also elucidate the role of the latter in assisting the effect of VSL on the redshift to manifest*. In Section IV we conduct an analysis of the Combined Pantheon Sample using our modified luminosity distance-vs-redshift formula derived in the preceding Section. In Section V we discuss the implications of our Pantheon analysis; in particular, we provide (i) a new interpretation of the accelerating expansion; and (ii) the potential explanation to the Hubble constant tension by way of the variation in the local scale of gravitationally-bound regions. Appendix A provides an alternative route to the modified Lemaitre redshift formula derived in Section III.

## II. THE MODIFIED ROBERTSON-WALKER METRIC

The Robertson-Walker (RW hereafter) metric starts with the assumption of homogeneity and isotropy of space. It also assumes the spatial component of the metric to be time-dependent. All of the time dependence is in the function  $a(t)$  known as the cosmic scale factor. The RW metric is the only one that is spatially homogeneous and isotropic. This is a geometrical result and is not tied to the equations of the gravitational field.

The RW metric has been determined to be:

$$ds^2 = c^2 dt^2 - a^2(t) \left[ \frac{dr^2}{1 - kr^2} + r^2 d\Omega^2 \right] \quad (1)$$

$$d\Omega^2 = d\theta^2 + \sin^2 \theta d\phi^2 \quad (2)$$

where the global cosmic scale factor  $a(t)$  is a function of the cosmic time  $t$  only (with  $a(t_0) = 1$  at our current time  $t_0$ ), and  $k$  the curvature determining the shape of the universe (open/flat/closed for  $k > 0, k = 0, k < 0$  respectively). The quantity  $c$  in the RW metric is taken to be the velocity of light  $c$  in Einstein's underlying theory; the latter  $c$  is an invariant (i.e., unaffected under a general coordinate transformation) but in principle can vary on the manifold. In the language of geometry,  $c$  can be a scalar field, rather than a universal constant.

When allowing for the variation in the velocity of light on the manifold, we retain the homogeneity and isotropy of space. In Barrow's VSL form [1], the velocity of light is a function of the scale factor, viz.

$$c = c_0 a^{-\zeta} \quad (3)$$

The RW metric remains applicable with only a minor modification being in the dependence of  $c$  on the scale factor. We thus arrive at the *modified* RW metric:

$$ds^2 = c^2(a) dt^2 - a^2(t) \left[ \frac{dr^2}{1 - kr^2} + r^2 d\Omega^2 \right] \quad (4)$$

$$= \frac{c_0^2}{a^{2\zeta}(t)} dt^2 - a^2(t) \left[ \frac{dr^2}{1 - kr^2} + r^2 d\Omega^2 \right] \quad (5)$$

in which  $c_0$  is the speed of light measured in the outer space region (which is subject to cosmic expansion) at our current time.

## III. MODIFYING REDSHIFT FORMULAE TO ENABLE VARIATION IN THE VELOCITY OF LIGHT

### A. Role of gravitationally-bound regions in detecting the redshift

The RW metric deals with the global cosmic scale factor. However, in order for an observer to detect the redshift,

the region containing the observer must not be directly subject to cosmic expansion.<sup>3</sup> Thanks to the attraction nature of gravity, regions that are populated with matter are expected to be able to resist cosmic expansion and retain their own local scale over the course of time since their formation post the recombination event. In order to understand the impact of variable velocity of light on the redshift, it is necessary for us to explicitly consider the local scale of gravitationally-bound regions. The reason is as follows.

A lightwave emitted from a supernova in a distant (gravitationally-bound) galaxy first has to transit into the outer space region which is not gravitationally-bound. It will then traverse the null geodesic of the RW metric and expands together with the cosmic factor  $a(t)$ . Finally, the lightwave must transit into the (gravitationally-bound) Milky Way to reach the astronomer's apparatus. Whereas the middle stage is well understood in standard cosmology, the first and the last stages have received little attention. It turns out that the first and the last stages are crucial in the context of VSL. This Section prepares the notations and concepts needed for our detailed examination in Section III B.

Figure 1 on Page 4 gives us a quick glimpse of the issue. On its way from a distant supernova to the Earth-based astronomer, the light ray must undergo 3 transits:

- Transit #1: from the *gravitationally-bound* galaxy (which contains the supernova) to the outer space region that encloses the emission galaxy.
- Transit #2: from the outer space region that encloses the emission galaxy to the outer space region that encloses the Milky Way. During Transit #2, the wavecrest follows the null geodesic of the RW metric and expands as a result of the cosmic expansion.
- Transit #3: from the outer space region that encloses the Milky Way into the *gravitationally-bound* Milky Way to finally reach the Earth-based observer.

As shown in Figure 1, let us denote:

- $a_e^{[loc]}$ , the local scale of the emission galaxy;
- $a_o^{[loc]}$ , the local scale of the Milky Way;
- $a_e$ , the global cosmic scale of the outer space region that encloses the emission galaxy;
- $a_o$ , the global cosmic scale of the outer space region that encloses the Milky Way;

in which the subscript “e” and “o” stand for “emission” and “observation” respectively, and the superscript  $[loc]$  means “local”. Note that, in principle,  $a_e^{[loc]}$  and  $a_o^{[loc]}$  may be *different*.

Likewise, let us denote:

- $\lambda_e^{[loc]}$ , the wavelength of the photon emitted by the supernova;
- $\lambda_o^{[loc]}$ , the wavelength of the photon detected by the observer;
- $\lambda_e$ , the wavelength of the photon in the outer space region that encloses the emission galaxy;
- $\lambda_o$ , the wavelength of the photon in the outer space region that encloses the Milky Way.

In addition,  $\lambda_o^*$  is the wavelength of the photon *if the source were to emit the photon at the observer's location*. It serves as a yardstick against which the Earth-based astronomer compares her detected wavelength  $\lambda_o^{[loc]}$  and produce the value of the redshift. In standard cosmology:

$$\lambda_o^* = \lambda_e^{[loc]} \quad (6)$$

In the context of VSL, it is possible and necessary to set  $\lambda_o^*$  and  $\lambda_e^{[loc]}$  apart. We let  $\lambda_o^*$  be related to  $\lambda_e^{[loc]}$  via the local scale of the emission galaxy and that of the Milky Way per the following relation:

$$\frac{\lambda_o^*}{\lambda_e^{[loc]}} = \frac{a_o^{[loc]}}{a_e^{[loc]}} \quad (7)$$

As will become clear in Section V B, by making the local scale of the emitter,  $a_e^{[loc]}$ , be dependent on its redshift  $z$  and exploiting Relation (7), we would obtain a potential explanation to the Hubble constant tension (i.e, the discrepancy in the estimates of  $H_0$  from late-time objects [21–23] versus from the Cosmic Microwave Background [24–33]). This is a by-product benefit of our analysis.

Finally, the Earth-based astronomer measures  $\lambda_o^{[loc]}$  then compares it with  $\lambda_o^*$  to obtain the value of the redshift:

$$z := \frac{\lambda_o^{[loc]} - \lambda_o^*}{\lambda_o^*} \quad (8)$$

## B. A refraction effect due to variable speed of light

In the VSL context depicted in Fig. 1, we further denote:

- $c_e^{[loc]}$ , the speed of light inside the emission galaxy (which has the local factor  $a_e^{[loc]}$ );

<sup>3</sup> If the Solar System had expanded together with the cosmos, the observer's apparatus would also have expanded in sync with the wavelength of the light ray emitted from a distant supernova and could not have detected any redshift.

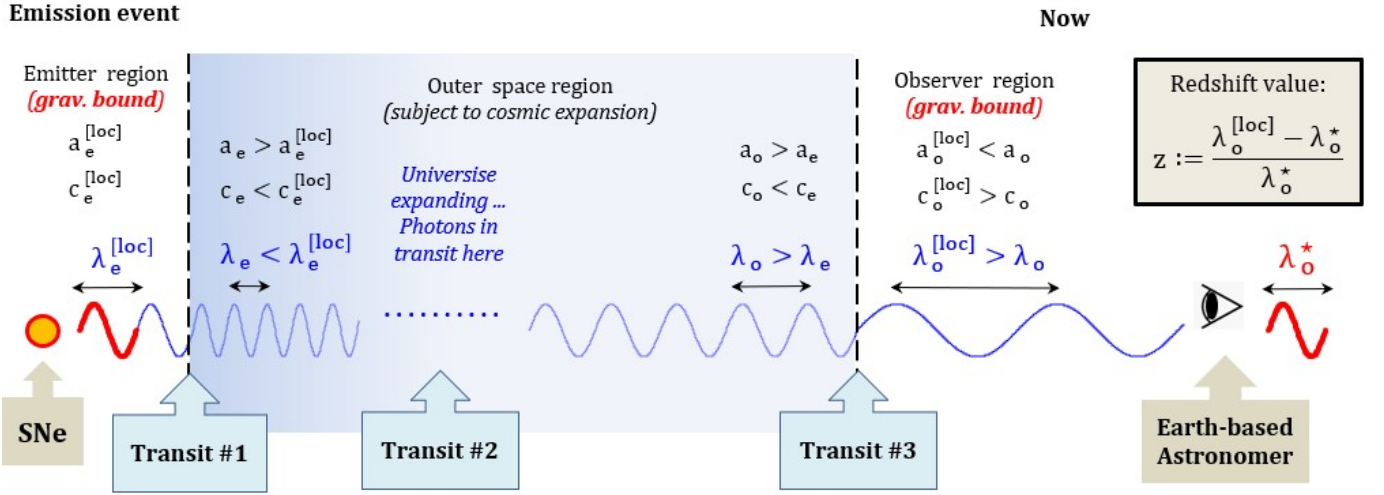


Figure 1: Demonstrating the case of  $c \propto a^{-1/2}$ . A lightwave from a supernova emission (shown on the far left) will have made 3 transits to reach the Earth-based astronomer (shown on the far right). In Transit #1, the lightwave exits the (gravitationally-bound) emission galaxy to enter the outer space region that surrounds the emission galaxy; the wavecrest gets compressed as light slows down. During Transit #2, the lightwave travels in the outer space which undergoes a cosmic expansion; as a result, the lightwave expands. In Transit #3, the lightwave enters the (gravitationally-bound) Milky Way; the wavecrest expands further as light speeds up. The Earth-based astronomer measures  $\lambda_o^{[loc]}$  and compares it with the yardstick  $\lambda_o^*$  in order to produce the redshift value (shown in the upper right corner box).

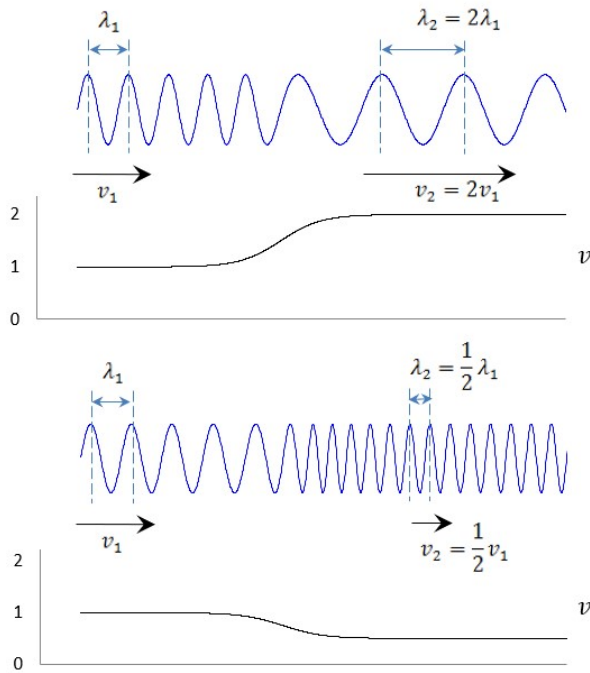


Figure 2: Change in wavelength as a wave travels in medium with varying speed of wave. Upper panel: as its speed doubles, so does its wavelength. Lower panel: wavelength halves as its speed halves, so does its wavelength. In either case, wavelength and velocity are proportional:  $\lambda_2/v_2 = \lambda_1/v_1$ .

- $c_o^{[loc]}$ , the speed of light inside the Milky Way (which has the local factor  $a_o^{[loc]}$ ). Note that  $c_o^{[loc]} = c_{SS} = 300,000 \text{ km/sec}$  is the speed of light measured in the Solar System where the astronomer lives. The “SS” in  $c_{SS}$  stands for “Solar System”.
- $c_e$ , the speed of light in the outer space region (which has the global factor  $a_e$ ) that encloses the emission galaxy;
- $c_o$ , the speed of light in the outer space region (which has the global factor  $a_o$ ) that encloses the Milky Way.

Let us start with a well-understood phenomenon: the behavior of a light ray in a medium with varying refractive index. It is well established that the wavelength of the light ray at a given location is proportional to the velocity of light at that location:

$$\lambda \propto v \quad (9)$$

Figure 2 illustrates the change in wavelength as a wave travels at varying velocity. In the upper panel, as the velocity increases, the front end of the wavecrest will rush forward leaving its back end behind thus stretching out the wavecrest. In the lower panel, the reverse situation occurs: as the velocity decreases, the front end of the wavecrest will slow down while its back end continues its course thus compressing the wavecrest. In either situation, the wavelength and the velocity of wave are directly

proportional:

$$\frac{\lambda_2}{\lambda_1} = \frac{v_2}{v_1} \quad (10)$$

For our problem at hand, the refraction phenomenon also applies to lightwaves which travel from a distant supernova toward the Earth-based astronomer. Figure 1 illustrates the essence of the refraction effect. It shows how the wavelength observed on Earth acquires an extra factor as compared with a classic case in which the speed of light is universal. For concreteness, Figure 1 demonstrates the example  $c \propto a^{-1/2}$ , namely, the speed of light decreases in reverse of the scale factor.

In Figure 1, as a light ray travels from distant SNe (far left) to Earth-based astronomer (far right), it passes through 4 regions, each one having its own scale and velocity of light. The 4 regions are:

- 1) The (gravitationally-bound) emission galaxy: scale  $a_e^{[loc]}$  and velocity of light  $c_e^{[loc]}$ . The photon emitted at this event has wavelength  $\lambda_e^{[loc]}$ .
- 2) The outer space region enclosing the emission galaxy: scale  $a_e$  and velocity of light  $c_e$ . The outer space region is subject to cosmic expansion. Since the outer space region might already have expanded before the SNe emits the light ray, in general:

$$a_e \geq a_e^{[loc]} \quad (11)$$

- 3) The outer space region enclosing the Milky Way: scale  $a_o$  and velocity of light  $c_o$ . As a result of cosmic expansion, the following inequality holds:

$$a_o > a_e \quad (12)$$

- 4) Inside the (gravitationally-bound) Solar System where the Earth-based observer resides: scale  $a_o^{[loc]}$  and velocity of light  $c_o^{[loc]}$ . Note that it is  $c_o^{[loc]} = c_{SS} = 300,000 \text{ km/sec}$ , with “SS” in  $c_{SS}$  short-handling for “Solar System”. As such, the following inequality holds:

$$a_o^{[loc]} < a_o \quad (13)$$

As a concrete example, Figure 1 sets  $a_e = 3 a_e^{[loc]}$ ;  $a_o = 2 a_e$ ;  $a_o^{[loc]} = \frac{1}{6} a_o$ . In this example,  $a_o^{[loc]} = a_e^{[loc]}$ .

The lightwave from a supernova must make 3 transits before reaching the Earth-based astronomer.

#### Transit #1:

The lightwave exits the emission galaxy (which is gravitationally-bound) to enter the outer space region (which is subject to cosmic expansion) that surrounds

the emission galaxy. During Transit #1, the wavecrest gets compressed as light slows down, viz.  $c_e < c_e^{[loc]}$  due to  $a_e > a_e^{[loc]}$ . In Fig. 1,  $a_e = 3 a_e^{[loc]}$  leading to  $c_e = \frac{1}{\sqrt{3}} c_e^{[loc]}$  per  $c \propto a^{-1/2}$ , and  $\lambda_e = \frac{1}{\sqrt{3}} \lambda_e^{[loc]}$  as a result of the refraction effect per  $\lambda \propto c$ .

#### Transit #2:

The lightwave traverse the null geodesic of the RW metric, from the outer space region that encloses the emission galaxy to the outskirts of the Milky Way. During Transit #2, the wavecrest gets stretched out as a result of the cosmic expansion:  $a_o > a_e$ . In Fig. 1,  $a_o = 2 a_e$  leading to  $c_o = \frac{1}{\sqrt{2}} c_e$  per  $c \propto a^{-1/2}$ , and  $\lambda_o = 2 \lambda_e$  resulting from the cosmic expansion.

#### Transit #3:

From the outskirts of the Milky Way, the lightwave enters the Milky Way (which is gravitationally-bound) and finally reaches the Earth-based observer. During Transit #3, the wavecrest gets stretched out further as the light speed increases:  $c_o^{[loc]} > c_o$  due to  $a_o^{[loc]} < a_o$ . In Fig. 1,  $a_o^{[loc]} = \frac{1}{6} a_o$  leading to  $c_o^{[loc]} = \sqrt{6} c_o$  per  $c \propto a^{-1/2}$ , and  $\lambda_o^{[loc]} = \sqrt{6} \lambda_o$  as a result of the refraction effect per  $\lambda \propto c$ .

#### The net effect:

The Earth-based astronomer compares her observation  $\lambda_o^{[loc]}$  with  $\lambda_o^*$  both of which are *directly measurable* by the astronomer. She would find that  $\lambda_o^{[loc]} = \sqrt{6} \lambda_o = \sqrt{6} \times 2 \lambda_e = \sqrt{6} \times 2 \times \frac{1}{\sqrt{3}} \lambda_e^{[loc]} = 2^{3/2} \lambda_e^{[loc]}$ . Note that in this example:  $\lambda_o^* = \lambda_e^{[loc]}$  because  $a_o^{[loc]} = a_e^{[loc]}$ . The astronomer would thus find that  $\lambda_o^{[loc]} = 2^{3/2} \lambda_o^*$ .

Note that in standard cosmology, the astronomer would only find that  $\lambda_o^{[loc]} = 2 \lambda_o^*$  which is a direct result of the cosmic expansion, viz.  $a_o = 2 a_e$ , taking place during Transit #2. In standard cosmology, as light speed is non-varying, Transit #1 and Transit #3 do not affect the wavelength of the light ray.

The Earth-based astronomer measures  $\lambda_o^{[loc]}$  then compares it with  $\lambda_o^*$  to obtain the value of the redshift:

$$z := \frac{\lambda_o^{[loc]} - \lambda_o^*}{\lambda_o^*} \quad (14)$$

In the example depicted in Fig. 1, the astronomer thus obtains a redshift value of  $z_{VSL} = 2^{3/2} - 1 \approx 1.82$ . In the absence of VSL, she would obtain a redshift value of  $z_{standard} = 2 - 1 = 1$  only.

Generally speaking, for a decreasing function of  $c$  w.r.t. the scale factor  $a$ , the VSL yields a larger redshift than

what is produced in standard cosmology. In the context of VSL, the change in the redshift therefore warrants a revision in the distance-vs-redshift relations, the topics we shall expound in the rest of this Section.

### C. Modifying Lemaître's formula

What is most interesting in the demonstration in Figure 1 is that the stretching out of the wavecrest during Transit #3 does *not* cancel out the compression of the wavecrest during Transit #1. The refraction occurring at Transit #1 and the "reverse" refraction taking place at Transit #3 do not net each other out. For a decreasing function of  $c$ , the net effect increases the value of  $z$  and results in a new formula for the redshift. Below is our derivation.

Due to the refraction effect at Transit #1:

$$\lambda_e = \lambda_e^{[loc]} \frac{c_e}{c_e^{[loc]}} \quad (15)$$

Due to the cosmic expansion during Transit #2:

$$\lambda_o = \lambda_e \frac{a_o}{a_e} \quad (16)$$

Due to the "reverse" refraction effect at Transit #3:

$$\lambda_o^{[loc]} = \lambda_o \frac{c_o^{[loc]}}{c_o} \quad (17)$$

Combining (15-17), we have:

$$\lambda_o^{[loc]} = \lambda_e^{[loc]} \frac{c_e}{c_e^{[loc]}} \cdot \frac{a_o}{a_e} \cdot \frac{c_o^{[loc]}}{c_o} \quad (18)$$

Further combining it with the yardstick, viz. (7), and the definition of the redshift in (8), we have:

$$1 + z := \frac{\lambda_o^{[loc]}}{\lambda_o^*} \quad (19)$$

$$= \frac{\lambda_o^{[loc]}}{\lambda_e^{[loc]}} \cdot \frac{\lambda_e^{[loc]}}{\lambda_o^*} \quad (20)$$

$$= \left( \frac{c_e}{c_e^{[loc]}} \cdot \frac{a_o}{a_e} \cdot \frac{c_o^{[loc]}}{c_o} \right) \frac{a_e^{[loc]}}{a_o^{[loc]}} \quad (21)$$

$$= \left( \frac{c_e}{c_o} \cdot \frac{a_o}{a_e} \right) \left( \frac{c_o^{[loc]}}{c_e^{[loc]}} \cdot \frac{a_e^{[loc]}}{a_o^{[loc]}} \right) \quad (22)$$

In [1], Barrow considered the VSL functional form:

$$c \propto a^{-\zeta} \quad (23)$$

which does not have a preferred scale. What is new in our approach is that we enable Barrow's functional form

for both types of scale factor, whether it is global and local.<sup>4</sup>

Applying (23) for the global scale, we obtain:

$$\frac{c_e}{c_o} = \left( \frac{a_e}{a_o} \right)^{-\zeta} \quad (24)$$

Likewise, applying (23) to the local scale, we obtain:

$$\frac{c_o^{[loc]}}{c_e^{[loc]}} = \left( \frac{a_o^{[loc]}}{a_e^{[loc]}} \right)^{-\zeta} \quad (25)$$

Combining (22), (24), and (25), we arrive at the *modified* Lemaître redshift formula:

$$1 + z = \left( \frac{a_e}{a_o} \right)^{-(1+\zeta)} \left( \frac{a_e^{[loc]}}{a_o^{[loc]}} \right)^{1+\zeta} \quad (26)$$

In (26),  $a_e^{[loc]}$  is a function of the redshift  $z$  of the emission galaxy. But it may also contains the idiosyncratic characters of the emission galaxy. Eq. (26) is thus understood in the "average" sense in which the idiosyncratic is being "averaged" out. Let us define a new quantity:

$$F(z) := \frac{a_e^{[loc]}}{a_o^{[loc]}} \quad (27)$$

which is a function of  $z$ . The *modified* Lemaître redshift formula is (setting  $a_o = 1$ ):

$$1 + z = a_e^{-(1+\zeta)} F^{1+\zeta}(z) \quad (28)$$

The quantity  $F(z)$  should be a monotonic and slowly-decreasing function w.r.t.  $z$ , satisfying  $F(z=0) = 1$ .

In the absence of the variation in the local scale, viz.  $F(z) \equiv 1 \forall z$ , the modified Lemaître redshift formula is simplified to:

$$1 + z = a_e^{-(1+\zeta)} \quad (29)$$

which is fundamentally *different* from the classic Lemaître redshift formula  $1 + z = a_e^{-1}$ .

The VSL exponent  $\zeta$  thus has come to the fore: via Eq. (29) it enforces major revisions in the distance-redshift

<sup>4</sup> The scale factor can be made tightly related to the (Ricci) scalar curvature. In such a scenario, the speed of light is directly determined by the Ricci scalar, both of which are invariants. This is the topics of our follow-up theoretical report [34]. This result translates into our current report that the applicability of (23) is non-discriminatory, regardless of whether the scale factor is global or local.

relations and warrants a new analysis for the Type Ia SNe data.<sup>5</sup>

Let us conclude this subsection by commenting on the oversight in previous analyses to date [12–14]. In these works, it was correctly observed that Eq. (16) is valid regardless of whether or not the speed of light varies during Transit #2. However, this fact alone is not sufficient for the conclusion (used in [12–14]) that the classic Lemaître redshift formula, viz.  $1 + z = a^{-1}$ , should remain valid for VSL. The reason is that  $\lambda_o$  is *not* what the Earth-based astronomer observes. To reach the astronomer, the lightwave needs to enter the Milky Way which has a scale *smaller* than the current global cosmic scale because the Milky Way has resisted the cosmic expansion. Since  $c \propto a^{-\zeta}$ , the velocity of light  $c_o^{[loc]}$  inside the Milky Way is *different* from the velocity of light  $c_o$  in the outer space region that encloses the Milky Way. The lightwave thus gets refracted during its entry to the Milky Way with its wavelength getting altered to  $\lambda_o^{[loc]} = \lambda_o c_o^{[loc]}/c_o$  per Eq. (17). It is the wavelength  $\lambda_o^{[loc]}$  that gets measured in the astronomer’s apparatus.

The novelty of our work is in our exposition of the VSL exponent  $\zeta$  in the modified Lemaître redshift formula, (28) or (29).

#### D. Modifying the distance-redshift formula

To ease the notation, from here on, we shall drop the subscript “e” and simply write  $a$  for  $a_e$ ,  $a^{[loc]}$  for  $a_e^{[loc]}$ ,  $c$  for  $c_e$ ,  $c^{[loc]}$  for  $c_e^{[loc]}$ . Likewise, we shall write  $a_o$  for  $a_o$  (which is conveniently set to 1),  $a_{SS}$  for  $a_o^{[loc]}$ ,  $c_o$  for  $c_o$ ,  $c_{SS}$  for  $c_o^{[loc]}$  (note:  $c_{SS} = 300,000 \text{ km/sec}$ ) with “SS” standing for “Solar System”.

In this subsection, we shall derive the distance-redshift formula applicable for VSL. To proceed, we shall adopt an evolution of the cosmic scale factor in the functional form:

$$a(t) = \left(\frac{t}{t_0}\right)^\mu \quad (30)$$

with  $a(t_0)$  being set equal 1. This functional form has no preferred scale. It covers the critical mode of expansion for the flat  $\Lambda$ CDM universe when  $\mu = 2/3$ . Taking

derivative of (30), we obtain the Hubble “constant”:

$$H(t) := \frac{\dot{a}}{a} = \frac{\mu}{t} \quad (31)$$

from which, the cosmic age is:

$$t_0 = \frac{\mu}{H_0} \quad (32)$$

whereas the total “proper length” is:

$$\begin{aligned} s_0 &= \int_0^{t_0} dt c(a) = c_0 \int_0^{t_0} dt a^{-\zeta} \\ &= c_0 \int_0^{t_0} dt \left(\frac{t}{t_0}\right)^{-\zeta\mu} = \frac{1}{1-\zeta\mu} c_0 t_0 \end{aligned} \quad (33)$$

Some useful rearrangement:

$$\frac{\dot{a}}{a} = H = \frac{\mu}{t} = \frac{\mu}{t_0} \frac{t_0}{t} = H_0 \frac{1}{a^{1/\mu}} \quad (34)$$

From (3) and (4) with  $k = 0$ , the coordinate distance in the almost flat space is:

$$r \approx \int_{t_e}^{t_o} \frac{c(a) dt}{a(t)} = c_0 \int_{t_e}^{t_o} \frac{dt}{a^{1+\zeta}(t)} \quad (35)$$

From the modified Lemaître redshift formula (28), we get:

$$dz = -(1+\zeta) \frac{\dot{a}}{a^{2+\zeta}} F^{1+\zeta}(z) dt \quad (36)$$

or

$$\frac{dt}{a^{1+\zeta}} = -\frac{1}{1+\zeta} \frac{dz}{\dot{a}/a} F^{-(1+\zeta)}(z) \quad (37)$$

in which we assume that  $\dot{a}^{[loc]}/a^{[loc]} \ll \dot{a}/a$ . Eq. (35) becomes:

$$\begin{aligned} r &= \frac{c_0}{1+\zeta} \int_0^z \frac{dz'}{(\dot{a}/a)(z')} F^{-(1+\zeta)}(z') \\ &= \frac{c_0}{(1+\zeta)H_0} \int_0^z dz' a^{1/\mu} F^{-(1+\zeta)}(z') \end{aligned} \quad (38)$$

Combined with the modified Lemaître redshift formula (28), the integrand in (38) is transformed to:

$$a^{1/\mu} F^{-(1+\zeta)} = \left[ a^{1+\zeta} F^{-(1+\zeta)} \right]^{\frac{1}{\mu(1+\zeta)}} F^{\frac{1}{\mu} - (1+\zeta)} \quad (39)$$

Let us define a new parameter  $\epsilon$  from  $\zeta$  and  $\mu$ :<sup>6</sup>

$$1 + \epsilon := \frac{1}{\mu(1+\zeta)} \quad (41)$$

<sup>6</sup> The total “proper length” in (33) can be re-expressed as:

$$s_0 = \frac{1}{\mu + \epsilon/(1+\epsilon)} c_0 t_0 \quad (40)$$

If  $\epsilon = 0$ , from (32), the total “proper length” further becomes  $\frac{1}{\mu} c_0 t_0 = \frac{c_0}{H_0} \equiv l_{Hubble}$  which is the Hubble length, defined using today’s speed of light  $c_0$ .

<sup>5</sup> Let us verify the demonstration in Figure 1 in the light of Formula (29). In Figure 1,  $c$  varies as  $a^{-1/2}$  (thus  $\zeta = 1/2$ ) and the universe has expanded by a factor of 2, viz.  $a_o = 2a_e$ . Equivalently,  $a \equiv a_e = 1/2$  (recalling that  $a_o = 1$ ). Formula (29) produces a redshift  $z = (1/2)^{-3/2} - 1 \approx 1.82$  in agreement with the value of  $z_{VSL}$  reported in the last paragraph of Section III B.

or, equivalently:

$$\frac{1}{\mu} - (1 + \zeta) = \epsilon (1 + \zeta) \quad (42)$$

upon which Eq. (39) can be conveniently recast, with the aid of (28), as:

$$\begin{aligned} a^{1/\mu} F^{-(1+\zeta)} &= \left[ a^{1+\zeta} F^{-(1+\zeta)} \right]^{1+\epsilon} F^{\epsilon(1+\zeta)} \\ &= \frac{1}{(1+z)^{1+\epsilon}} F^{\epsilon(1+\zeta)} \end{aligned} \quad (43)$$

By virtue of Eqs. (38) and (43), we then obtain the *modified* distance-redshift relation:

$$\frac{r}{c_0} = \frac{1}{(1+\zeta) H_0} \int_0^z dz' \frac{F^{\epsilon(1+\zeta)}(z')}{(1+z')^{1+\epsilon}} \quad (44)$$

or, upon applying the age formula (32):

$$\frac{r}{c_0} = t_0 (1 + \epsilon) \int_0^z dz' \frac{F^{\frac{\epsilon}{\mu(1+\epsilon)}}(z')}{(1+z')^{1+\epsilon}} \quad (45)$$

In the limit  $\epsilon \rightarrow 0$ ,  $F(z)$  disappears from the integrand in Eq. (45), and the coordinate distance is vastly simplified to:

$$\frac{r}{c_0} = t_0 \ln(1+z) \quad (46)$$

In the limit  $\epsilon \rightarrow 0$ , the two exponents  $\zeta$  and  $\mu$  are directly related:

$$1 + \zeta = \frac{1}{\mu} \quad (47)$$

For the sake of comparison, we cite the  $\Lambda$ CDM distance-redshift relation (with  $\Omega_{curv} = 0$ ):

$$\frac{r}{c} = \frac{1}{H_0} \int_0^z \frac{dz'}{\sqrt{\Omega_M(1+z')^3 + \Omega_\Lambda}} \quad (48)$$

and that of the flat CDM model ( $\Omega_M = 1$ ,  $\Omega_\Lambda = 0$ ,  $\Omega_{curve} = 0$ ):

$$\frac{r}{c} = \frac{2}{H_0} \left( 1 - \frac{1}{\sqrt{1+z}} \right) \quad (49)$$

### E. Modifying the luminosity distance-redshift formula

As in standard cosmology, the luminosity distance  $d_L$  is defined via the absolute luminosity  $L$  and the apparent luminosity  $J$ :

$$d_L^2 = \frac{L}{4\pi J} \quad (50)$$

On the other hand, the absolute luminosity  $L$  and the apparent luminosity  $J$  are related:

$$4\pi r^2 J = L \frac{\lambda_o^{[loc]}}{\lambda_e^{[loc]}} \cdot \frac{\lambda_o^{[loc]}}{\lambda_e^{[loc]}} \quad (51)$$

In the RHS of (51), the first term  $\lambda_o^{[loc]}/\lambda_e^{[loc]}$  represents the “loss” in the energy of the red-shifted photon known as the “Doppler theft”. The second (identical) term  $\lambda_o^{[loc]}/\lambda_e^{[loc]}$  is due to the dilution factor in the photon density as the same number of photons get distributed in a prolonged wavecrest in the radial direction (i.e., the light ray). The  $4\pi r^2$  in the LHS of (51) is the spherical dilution in flat space. From (50) and (51), we have:

$$d_L = r \frac{\lambda_o^{[loc]}}{\lambda_e^{[loc]}} \quad (52)$$

In terms of the redshift (8) and the yardstick (7), the luminosity distance is:

$$d_L = r \frac{\lambda_o^{[loc]}}{\lambda_o^*} \cdot \frac{\lambda_o^*}{\lambda_e^{[loc]}} = r (1+z) \frac{a_o^{[loc]}}{a_e^{[loc]}} \quad (53)$$

or, by including (27):

$$d_L = r (1+z) \frac{1}{F(z)} \quad (54)$$

Due to the refraction effect at Transit #3, the apparent luminosity distance observed by the Earth-based astronomer  $d_L^{[loc]}$  differs from  $d_L$  by the factor  $c_{SS}/c_0$ , viz.

$$\frac{d_L^{[loc]}}{c_{SS}} = \frac{d_L}{c_0} \quad (55)$$

Finally, combining with (45), we obtain the *modified* luminosity distance-redshift relation:

$$\frac{d_L^{[loc]}}{c_{SS}} = \frac{t_0(1+\epsilon)}{F(z)} (1+z) \int_0^z dz' \frac{F^{\frac{\epsilon}{\mu(1+\epsilon)}}(z')}{(1+z')^{1+\epsilon}} \quad (56)$$

This is the central formula of our approach to assess Type Ia supernovae data, to be conducted in Section IV A. Formula (56) contains 3 parameters:  $t_0$ ,  $\epsilon$  and  $\mu$ , and involves a function  $F(z)$  which captures the dependence of the local scale of gravitationally-bound regions on the redshift. The function  $F$  cannot be determined from the Friedmann equations which deal only with the global cosmic scale factor. It would require separate modeling.

One potential candidate for the variation of the local scale as a function of redshift is the following function:

$$F(z) := F_\infty + (1 - F_\infty) \frac{2}{1 + e^{\kappa z}} \quad (57)$$

This parsimonious choice ensures that  $F(z)$  is a monotonic slowly-varying function, satisfying  $F(z=0) = 1$ . The function in (57) has 2 parameters:  $F_\infty$  which is the saturation value of  $F$  at high- $z$  and  $\kappa$  which specifies the crossover point between low- $z$  and high- $z$ .

For completeness, we cite the standard luminosity distance-redshift relation (with  $\Omega_{curv} = 0$ ):

$$\frac{d_L}{c} = \frac{1}{H_0} (1+z) \int_0^z \frac{dz'}{\sqrt{\Omega_M(1+z')^3 + \Omega_\Lambda}} \quad (58)$$



and that in the flat CDM model ( $\Omega_M = 1, \Omega_\Lambda = 0, \Omega_{curve} = 0$ ):

$$\frac{d_L}{c} = \frac{2}{H_0}(1+z) \left(1 - \frac{1}{\sqrt{1+z}}\right) \quad (59)$$

Note that the flat CDM model (59) is a special case of our VSL formula (56) when  $\epsilon = 1/2$ ,  $\mu = 2/3$  (hence  $\zeta = 0$  per (41)) and  $F(z) \equiv 1 \forall z$ , and by virtue of  $t_0 = 2/(3H_0)$ .

#### IV. FITTING OF THE MODIFIED REDSHIFT FORMULAE TO THE PANTHEON DATASET

##### A. General assessment

We are now well-equipped to assess the observational data of Type Ia supernovae [16–19]. Our numerical tool and the output of our analysis presented in this Section are available upon request.

In [16], Scolnic and collaborators produced a dataset of luminosity for 1,048 objects with redshift  $z$  ranging from 0.01 to 2.25. Their actual Combined Pantheon Sample is accessible in [17]. The observational data are given in the form of distance modulus  $\mu := m - M$  which is related to luminosity distance  $d_L$  as:

$$\mu := m - M = 5 \log_{10}(d_L/Mpc) + 25 \quad (60)$$

The Pantheon dataset provides, for each object  $i^{th}$ , the value of redshift  $z_i$ , the value of  $m_i$  together with its error bar  $\sigma_i$ . For each data point  $i^{th}$ , we add in a constant value of  $|M| = 19.35$  to recover the distance modulus  $\mu_i^{data}$ .

In Section III E we derived the modified luminosity distance-redshift formula in Barrow’s VSL context, Eq. (56), and proposed a minimal model for the variation in the local scale of gravitationally-bound regions, Eq. (57). The integral in (56) must be carried out via numerical means (tool available upon request). For each combination of  $\{t_0, \mu, \epsilon, F_\infty, \kappa\}$  we use Formula (56) in conjunction with (57) to compute the VSL “model” luminosity distance  $d_{L,i}^{[loc] model}$  for object  $i^{th}$  then convert it to  $\mu_i^{model}$  via Eq. (60). Our aim is to adjust the VSL model parameters in order to minimize the  $\chi^2$  of the difference between a model’s prediction  $\{\mu_i^{model}\}$  and the  $n = 1,048$  Pantheon data points  $\{\mu_i^{data}\}$  normalized by the measurement error  $\sigma_i$ :

$$\chi^2 := \frac{1}{n} \sum_{i=1}^n \frac{1}{\sigma_i^2} (\mu_i^{data} - \mu_i^{model})^2 \quad (61)$$

Figure 3 is the result of our fit presented in a 3-dimensional grid  $\{\mu, \epsilon, (1+\epsilon)t_0\}$ . Note that we arrange  $t_0$  and  $\epsilon$  in a combination  $(1+\epsilon)t_0$ . The parameter  $\mu$  takes in 3 values: 1/2, 2/3, 1. The range for  $\epsilon$  is from  $-0.5$  to 1. The range for  $(1+\epsilon)t_0$  is from 13 Gy to 15 Gy.

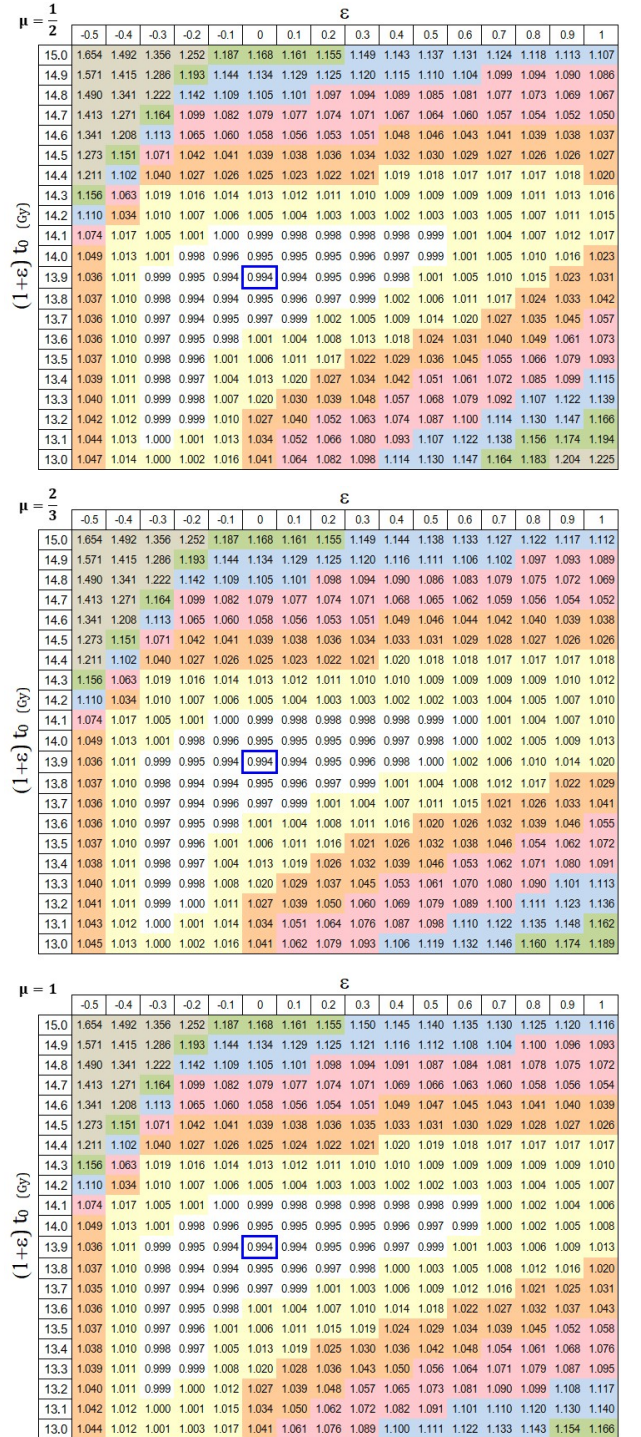


Figure 3: Value of  $\chi$  on a 3-d grid. From top to bottom:  $\mu = 1/2, 2/3, 1$  resp. Stratifying color:  $\chi < 1$  in white;  $\chi \in [1, 1.02]$  in yellow;  $\chi \in [1.02, 1.05]$  in orange;  $\chi \in [1.05, 1.1]$  in pink;  $\chi \in [1.1, 1.15]$  in blue;  $\chi \in [1.15, 1.2]$  in green;  $\chi \geq 1.2$  in gray. The grid point with lowest  $\chi$  is boxed in blue.

For each point on the grid  $\{\mu, \epsilon, (1+\epsilon)t_0\}$ , we minimize the  $\chi^2$  error by adjusting the two parameters  $(F_\infty, \kappa)$  of the function  $F(z)$ . Figure 3 shows the value of  $\chi$ , with

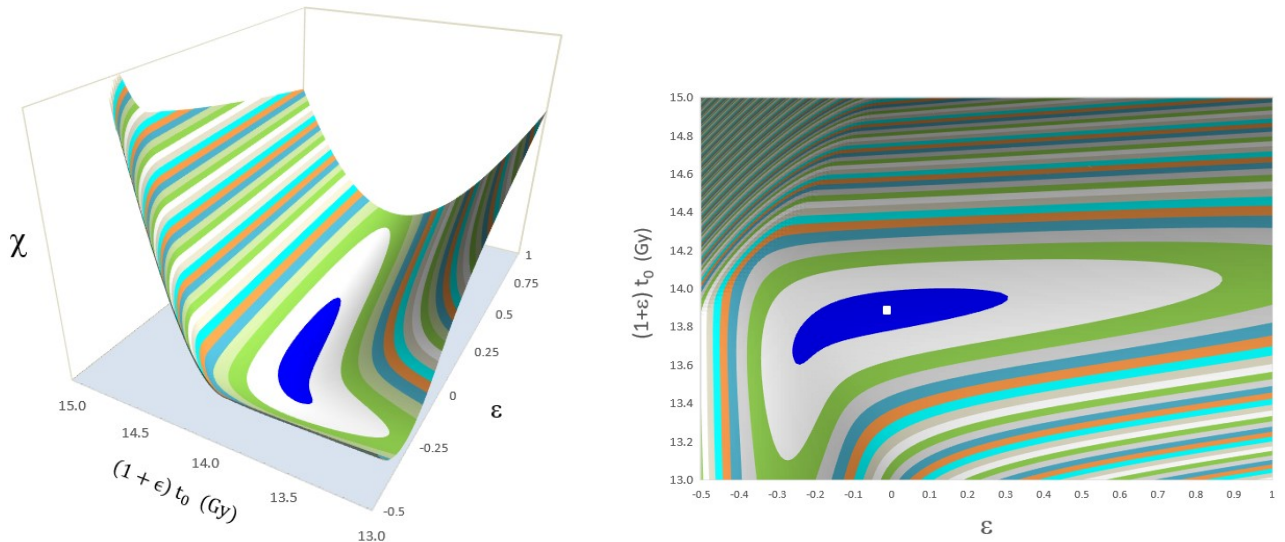


Figure 4: Contour plots of  $\chi$  for Formula (62) in fine resolution. The dark blue area has lowest  $\chi$  (smaller than 0.995). Each successive surrounding band has increasing  $\chi$  with width  $\Delta\chi = 0.005$ . The white dot in the right panel represents  $\chi_{min} \approx 0.993942$ , achieved at  $t_0 \approx 14.2$  Gy,  $\epsilon = -0.02$ ,  $F_\infty = 0.9$ ,  $\kappa = 5.4$ .

stratifying colors as explained in the caption.

The fit shows a very weak dependence of  $\chi$  on  $\mu$ . Across the 3 tables in Fig. 3, the variation in  $\chi$  is negligible. Note that the column with  $\epsilon = 0$  is identical for all 3 tables since for  $\epsilon = 0$  the parameter  $\mu$  would drop out of Formula (56).

The central area with  $\chi < 1$  shown in white gathers around  $(1+\epsilon)t_0 \approx 13.1\text{--}14.1$  Gy with  $\epsilon$  ranging from  $-0.3$  to  $0.6$ . The grid point with lowest  $\chi_{min} = 0.99395$  indicated in the blue box occurs at  $\{\epsilon^*, t_0^*\} = \{0, 13.9\text{ Gy}\}$  regardless of  $\mu$ .

Given that the effect of  $\mu$  is very weak, we also try with a simplified version of (56) by suppressing  $F(z)$  in the integrand to have a reduced formula:

$$\begin{aligned} \frac{d_L^{[loc]}}{c_{SS}} &= \frac{t_0(1+\epsilon)}{F(z)} (1+z) \int_0^z \frac{dz'}{(1+z')^{1+\epsilon}} \\ &= \frac{t_0(1+\epsilon)}{F(z)} (1+z) \frac{1}{\epsilon} \left[ 1 - \frac{1}{(1+z)^\epsilon} \right] \end{aligned} \quad (62)$$

We repeat the fit of the Pantheon data using Formula (62). Figure 4 shows the contour plots for  $\chi$  of this exercise. The overall minimum of  $\chi$  (shown by the white dot in the right panel) is achieved at  $t_0 \approx 14.2$  Gy,  $\epsilon = -0.02$ ,  $F_\infty = 0.9$ ,  $\kappa = 5.4$  which is very close to the vertical axis  $\epsilon = 0$ .

### B. Special case: Fitting for $\epsilon = 0$

The fit in Section IV A cannot reject the null hypothesis of  $\epsilon = 0$ . In what follows, we shall provide a theoretical justification in support of  $\epsilon = 0$ .

With the evolution rule (30) of the cosmic scale factor:

$$a \propto t^\mu \quad (63)$$

on the dimensionality ground, the speed of light should vary as:

$$c \propto \frac{a}{t} \propto a^{1-\frac{1}{\mu}} \quad (64)$$

Compared with (23),  $c \propto a^{-\zeta}$ , we have:

$$-\zeta = 1 - \frac{1}{\mu} \quad (65)$$

or

$$\mu(1+\zeta) = 1 \quad (66)$$

Combining (66) with the definition of  $\epsilon$  in (41), we arrive at:

$$\epsilon = 0 \quad (67)$$

In the rest of this subsection, we shall adopt  $\epsilon = 0$ . In this case, the luminosity distance-vs- $z$  (56) is vastly simplified to:

$$\frac{d_L^{[loc]}}{c_{SS}} = \frac{t_0}{F(z)} (1+z) \ln(1+z) \quad (68)$$

with  $\mu$  dropping out of the equation. Figure 5 plots  $\chi$  as a function of  $t_0$ , with  $\chi$  achieving the global minimum value of  $\chi_{VSL} = 0.99395$  at  $t_0^* = 13.9$  Gy,  $F_\infty^* = 0.894$ , and  $\kappa^* = 0.502$ . Also note that in Figure 5 for  $t_0 \gtrsim 14.8$ , with  $\kappa \rightarrow 0$ , by virtue of (57),  $F(z)$  would approach 1 for

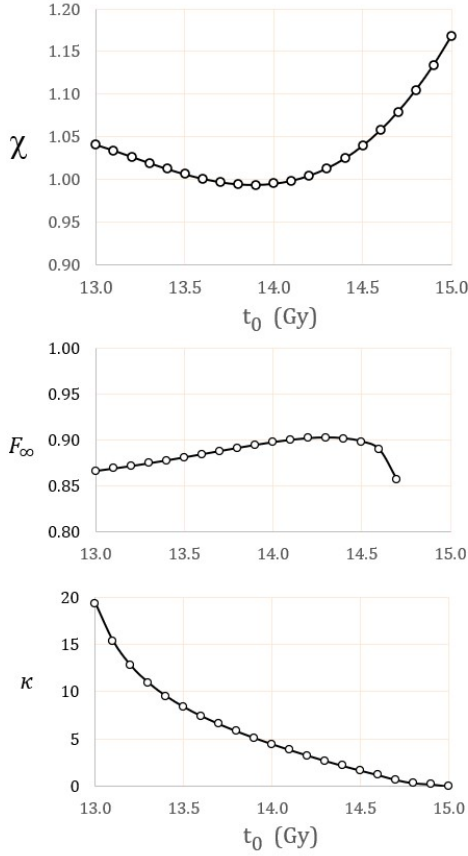


Figure 5: Special case:  $\epsilon = 0$ . Optimal values of  $\chi$ ,  $F_\infty$ , and  $\kappa$  as function of  $t_0$ .  $\chi$  reaches minimum at  $t_0^* \approx 13.9$  Gy.

all  $z$ , rendering  $F_\infty$  irrelevant. We thus do not show  $F_\infty$  in the right end of the middle plot.

At the optimal point  $\{t_0^*, F_\infty^*, \kappa^*\}$ , the variation in  $F$  as a function of redshift  $z$  is shown in the upper panel of Figure 6. Combining this knowledge of  $F(z)$  with Eq. (28), we produce the variation of  $F$  as a function of the cosmic scale factor presented in the lower panel of Figure 6 and the dependence of the cosmic scale factor in terms of redshift displayed in Figure 7. Also shown in Figure 7 is the classic Lemaître redshift formula.

Figure 8 displays the fits to our VSL model (solid curve) and to the  $\Lambda$ CDM (long-dashed curve), respectively. The best fits produce  $\chi_{VSL} = 0.99395$  for our VSL model (Formula (68) with  $t_0^* = 13.9$  Gy,  $F_\infty^* = 0.894$ ,  $\kappa^* = 5.202$ ) and  $\chi_{\Lambda CDM} = 0.99410$  for  $\Lambda$ CDM (Formula (58) with  $H_0 = 70.2$ ,  $\Omega_M = 0.285$ ,  $\Omega_\Lambda = 0.715$ ,  $\Omega_{curv} = 0$ ). The dotted curve corresponds the flat CDM model's Formula (59) with  $H_0 = 70.2$ . Figure 9 is identical to Figure 8 except that the Pantheon data points are removed for clarity. It is worth commenting that our VSL fit (solid curve) and the  $\Lambda$ CDM fit (long-dashed curve) are *indistinguishable* in Figures 8 and 9.

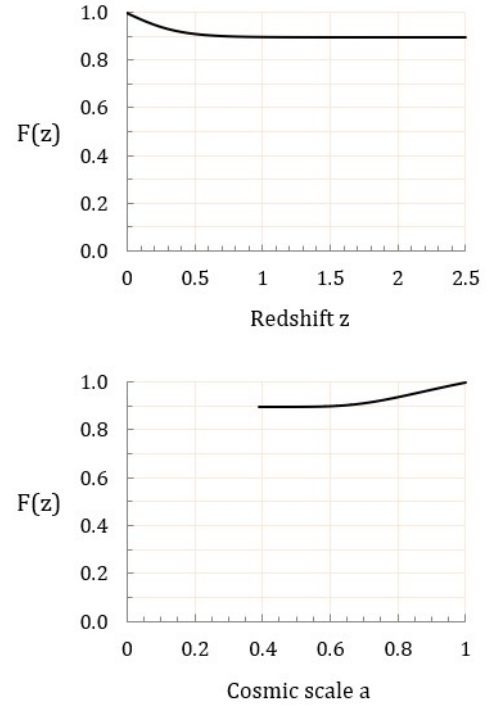


Figure 6: The variation of the local scale as functions of redshift (upper panel) and of cosmic scale factor (lower panel).

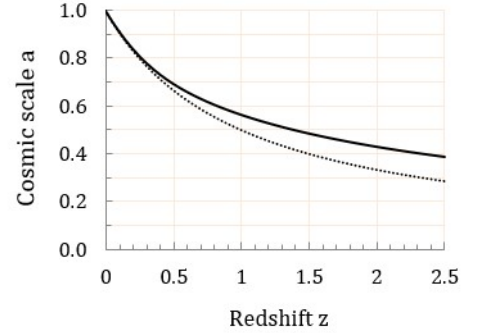


Figure 7: The variation of the global cosmic scale  $a$  as a function of redshift. Solid line: our VSL model with  $\zeta = 1/2$ . Dotted line: classic Lemaître's formula, viz.  $1 + z = a^{-1}$ .

To further probe the quality of the fits, we also compute the absolute moments of the normalized errors, defined as:

$$L_k := \left[ \frac{1}{n} \sum_{i=1}^n \frac{1}{\sigma_i^k} \left| \mu_i^{\text{data}} - \mu_i^{\text{model}} \right|^k \right]^{1/k} \quad (69)$$

which includes  $\chi$  as a special case,  $\chi \equiv L_2$ . If the normalized error  $(\mu_i^{\text{data}} - \mu_i^{\text{model}})/\sigma_i$  follows a Gaussian distribution of zero mean and unit variance, the analytical



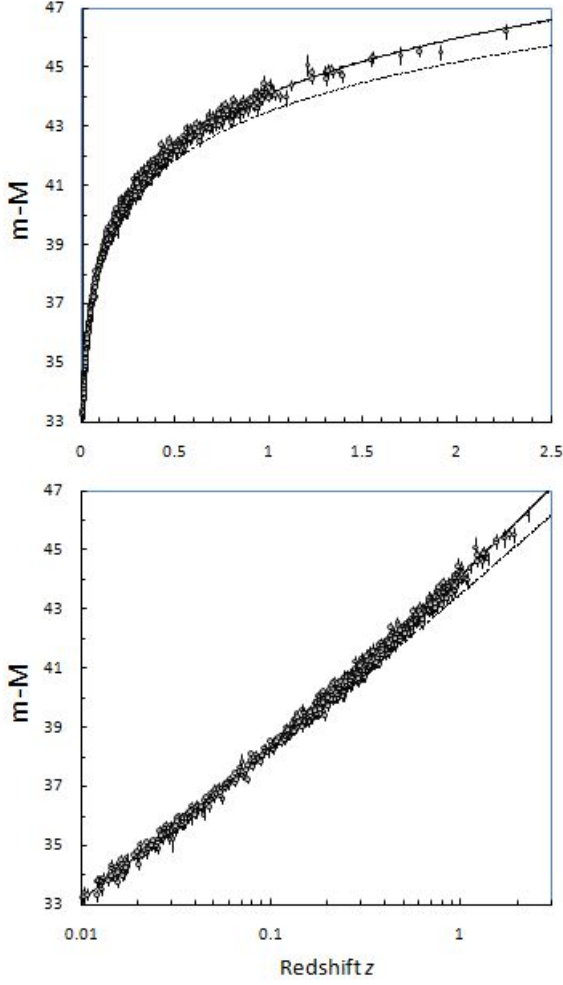


Figure 8: Comparison of various luminosity distance-redshift formulae fitted to the Pantheon data. Open circles: 1,048 Pantheon data points with error bars, listed in Ref. [17]. Long-dashed line:  $\Lambda$ CDM model's formula (58), with  $H_0 = 70.2$ ,  $\Omega_M = 0.285$ ,  $\Omega_\Lambda = 0.715$ ,  $\Omega_{curv} = 0$ . Dotted line: flat CDM model's formula (59), with  $H_0 = 70.2$ ,  $\Omega_M = 1$ ,  $\Omega_\Lambda = 0$ ,  $\Omega_{curv} = 0$ . Solid line: our VSL formulae (68) and (57) with  $t_0^* = 13.9$  Gy,  $F_\infty^* = 0.894$ ,  $\kappa^* = 5.202$ . Redshift shown in linear scale (upper panel) and in log scale (lower panel).

formula for its absolute moment of order  $k$  is:

$$L_k = \left[ \frac{1}{\sqrt{2\pi}} \int_{-\infty}^{\infty} dx |x|^k e^{-\frac{1}{2}x^2} \right]^{1/k} = \begin{cases} \left[ (k-1)!! \sqrt{\frac{2}{\pi}} \right]^{1/k} & \text{if } k \text{ odd} \\ [(k-1)!!]^{1/k} & \text{if } k \text{ even} \end{cases} \quad (70)$$

Figure 10 lists the absolute moments of our VSL, the  $\Lambda$ CDM, and the Gaussian analytic. Our VSL model is indistinguishable from the  $\Lambda$ CDM in terms of the absolute moments up to the order  $20^{th}$ .

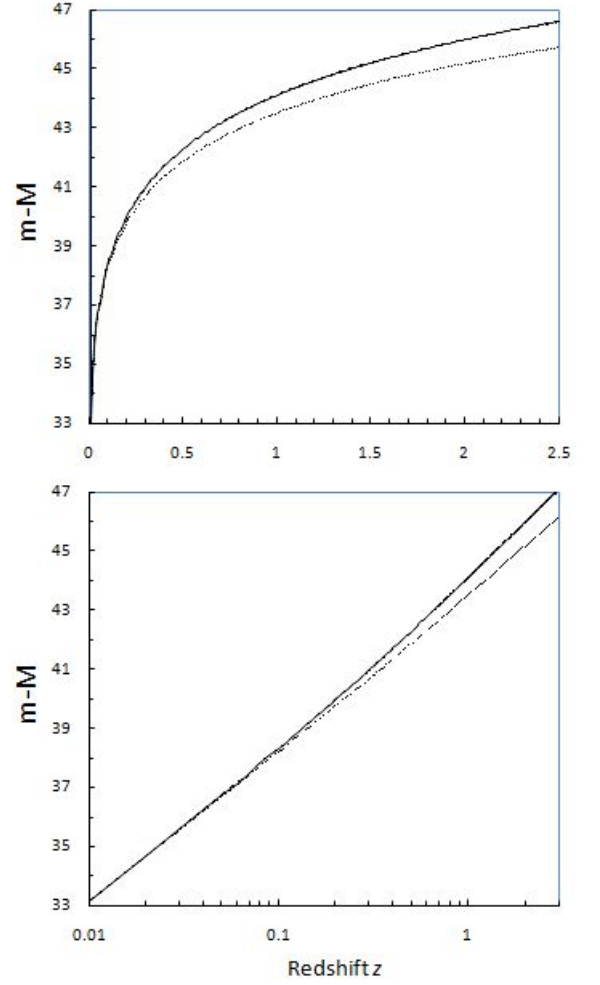


Figure 9: Same as Figure 8 but with the Pantheon data points removed for clarity. Our VSL model and the  $\Lambda$ CDM model are indistinguishable for all values of  $z \in (0, 2.25)$ .

k	Our VSL	LCDM	Analytic	k	Our VSL	LCDM	Analytic
1	0.76979	0.76958	0.79788	11	2.16327	2.16299	2.07460
2	0.99395	0.99410	1	12	2.23862	2.23791	2.16140
3	1.18570	1.18628	1.16858	13	2.30723	2.30602	2.24486
4	1.35570	1.35650	1.31607	14	2.36997	2.36820	2.32532
5	1.50894	1.50981	1.44879	15	2.42760	2.42522	2.40310
6	1.64768	1.64852	1.57042	16	2.48075	2.47772	2.47844
7	1.77312	1.77387	1.68333	17	2.52995	2.52624	2.55156
8	1.88627	1.88687	1.78916	18	2.57565	2.57124	2.62264
9	1.98823	1.98862	1.88909	19	2.61822	2.61311	2.69185
10	2.08017	2.08027	1.98401	20	2.65799	2.65217	2.75933

Figure 10: Goodness of fit for the absolute moments  $L_k$  up to order  $20^{th}$ . Definition of  $L_k$  is in Eq. (69), with analytic values given in Eq. (70).

The meaning and implications of  $F(z)$  will be discussed in Section V B. Although our VSL fit involves 3 adjustable parameters, the meaning of the 2 parameters ( $F_\infty$  and  $\kappa$ ) is intuitive and direct: they are to account for a variation of the local scale in the gravitationally-bound regions over the course of cosmic time.

## V. INTERPRETATIONS OF RESULTS

There are 2 agents at play in our VSL approach:

- #1) A variation in the velocity of light, characterized by the parameter  $\zeta$  (or equivalently  $\mu$  in the relation  $1 + \zeta = 1/\mu$ );
- #2) A variation in the local scale of gravitationally-bound regions, parameterized by  $F_\infty$  and  $\kappa$ .

We discuss the meaning and implications of each agent in this Section.

### A. A new interpretation of the acceleration in Type Ia SNe by way of VSL

We first focus on Agent #1. To do so, we disable Agent #2 by suppressing the variation in the local scale  $F(z)$  in Eq. (68) to obtain:

$$\frac{d_L^{[loc]}}{c_{SS}} = t_0 (1+z) \ln(1+z) \quad (71)$$

We then carry out a refit of the Pantheon dataset to Formula (71) which has only 1 free parameter,  $t_0$ . Note that  $\zeta$  is absent from this Formula. The result of the fit is displayed in Figure 11. The 1,048 Pantheon data points are shown in open circles with error bars. The solid line shows Formula (71) corresponding to one parameter  $t_0 = 14.7$  Gy with  $\chi_{min} = 1.1197$ . The long-dashed line corresponds to  $\Lambda$ CDM model's Formula (58) with 3 parameters  $H_0 = 70.2$ ,  $\Omega_M = 0.284$ ,  $\Omega_\Lambda = 0.716$ ,  $\Omega_{curv} = 0$  with  $\chi_{min} = 0.9941$ . The dotted line shows the flat CDM model's Formula (59) with  $H_0 = 70.2$ .

The most outstanding feature in Figure 11 is that in the high- $z$  section the solid curve (i.e., VSL model) with only 1 single adjustable parameter  $t_0$  acquires an upward slopping above the dotted curve (i.e., the flat CDM model). This upward slopping behavior of SNeIa has been interpreted as the hallmark of an acceleration in the recent epoch. Overall, the solid curve tracks the SNe data reasonably well; it closely resembles the long-dashed curve (i.e., the  $\Lambda$ CDM model) which has 3 adjustable parameters ( $H_0$ ,  $\Omega_M$ ,  $\Omega_\Lambda$ ). Also note that this “optimal” value of  $t_0 = 14.7$  Gy is not too far off from the value of  $t_0^* = 13.9$  Gy obtained via Formula (68) which activates the use of  $F(z)$ . Thus, even without allowing

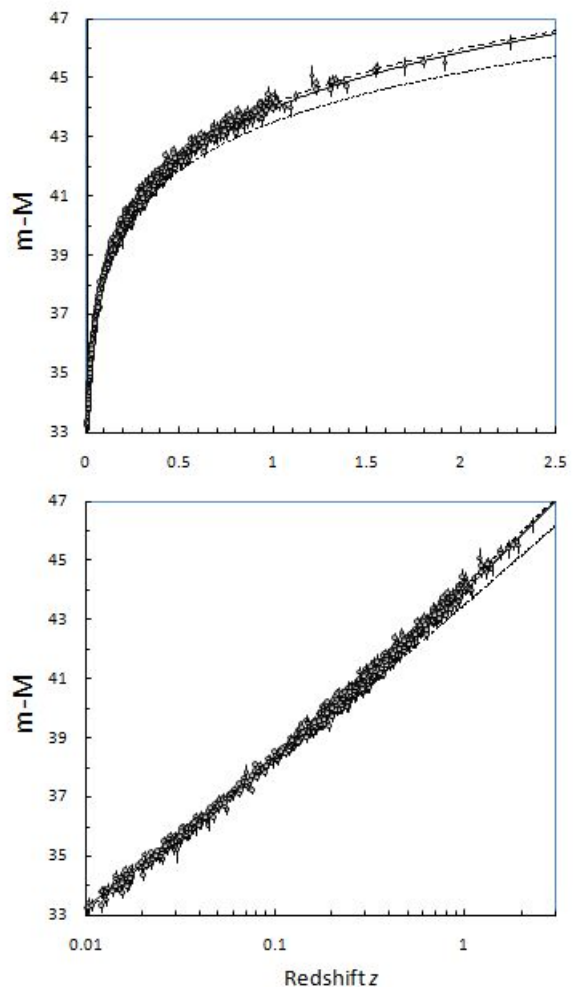


Figure 11: Fitting the Pantheon dataset with Formula (71) which deactivates the function  $F(z)$ . Open circles: 1,048 data points with error bars, listed in Ref. [17]. Solid line: VSL Formula (71) with  $t_0 = 14.7$  Gy. Long-dashed line:  $\Lambda$ CDM model Formula (58) with  $H_0 = 70.2$ ,  $\Omega_M = 0.284$ ,  $\Omega_\Lambda = 0.716$ . Dotted line: flat CDM model Formula (59) with  $H_0 = 70.2$ . Redshift shown in linear scale (upper panel) and in log scale (lower panel).

the variation in the local scale of gravitationally-bound regions, the variation in the velocity of light *alone* is already able to capture the behavior of the SNe data in the Pantheon Sample. In particular, the distance modulus  $\mu$  for the high- $z$  supernovae exceeds what would have been expected from the flat CDM model with  $H_0 = 70.2$  and tracks the  $\Lambda$ CDM model quite closely in both low- $z$  and high- $z$  sections. Whereas standard cosmology and the VSL approach each is able to account for the excess in  $\mu$  compared with the flat CDM model in the high- $z$  section, standard cosmology needs to resort to the cosmological component  $\Omega_\Lambda$ , whereas the VSL approach bypasses  $\Omega_\Lambda$ .

Parsimony asides, let us seek the intuition behind the accelerating expansion in Type Ia SNe in the light of

our VSL-based analysis. In our analysis, the Pantheon dataset is found to be consistent with a family of universes. In each member in the family, the mode of expansion is  $a \propto t^\mu$  and the light speed varies in the fashion  $c \propto a^{-\zeta}$  with  $\zeta = 1 - 1/\mu$  as dictated by Eq. (66). By itself, the Pantheon dataset is silent about the value of  $\mu$  (and  $\zeta$ ). We shall consider 2 most relevant modes of expansion in what follows.

*The linear expansion mode,  $a \propto t$*

This universe, with  $\mu = 1$ , corresponds to  $\zeta = 0$ ; namely, the speed of light is unchanged over the course of its expansion. In other words, the Pantheon data is consistent with a universe with linear expansion and a non-variable speed of light. In the later epoch, this mode of expansion is faster than the critical model in the flat CDM model,  $a \propto t^{2/3}$ . This means that, compared with the baseline case of  $a \propto t^{2/3}$ , this universe does accelerate.

*The critical expansion mode,  $a \propto t^{2/3}$*

This universe, with  $\mu = 2/3$ , corresponds to  $\zeta = 1/2$ ; namely, the speed of light decreases as the universe expands,  $c \propto a^{-1/2}$ . Let us deep dive into this very interesting case.

Consider two supernovae A and B at distances  $d_A$  and  $d_B$  away from the Earth such that  $d_B = 2d_A$ . In standard cosmology, their redshift values  $z_A$  and  $z_B$  are related:  $z_B \approx 2z_A$  (to the first-order approximation). However, this relation breaks down in the VSL context. In the VSL universe which accommodates the variation in the speed of light in the form  $c \propto a^{-1/2}$ , light had traveled faster in the distant past (when the cosmic factor  $a \ll 1$ ) than it did in the more recent epoch (when  $a \lesssim 1$ ). Therefore, the photon emitted from supernova B could cover twice as long the distance in less than twice the amount of time as would be required from the photon emitted from supernova A. Having spent less time in transit than what standard cosmology would have demanded, the B-photon experienced less cosmic expansion than expected, and thus experienced a lower redshift than the classic Lemaître formula would have required. Namely:

$$z_B < 2z_A \quad \text{for} \quad d_B = 2d_A \quad (72)$$

Conversely, consider a supernova C with  $z_C = 2z_A$ . In order for the C-photon to have experienced twice as much the redshift as the A-photon did, the C-photon must travel a distance exceeding twice as long compared with the A-photon:  $d_C > 2d_A$ . This is because since the C-photon traveled faster at the beginning of its journey toward Earth, it must start at a farther distance (thus appearing fainter than expected) to have experienced enough cosmic expansion and hence the redshift.

Namely:

$$d_C > 2d_A \quad \text{for} \quad z_C = 2z_A \quad (73)$$

Therefore, the distance-vs- $z$  plot gains an additional upward slope in the high- $z$  section, as is captured in the behavior of the solid curve in Figure 11. We conclude:

*For a universe which expands in the critical mode,  $a \propto t^{2/3}$ , the acceleration is equivalent to a variation in the velocity of light in the  $c \propto a^{-1/2}$  fashion.*

Recall that in 1911 during his search for a formulation of GR, Einstein originated the possibility of VSL [2–4]. He explicitly allowed the gravitational field to influence the *value* of the velocity of light; see Page 903 of Ref. [2]: “If  $c_0$  denotes the velocity of light at the coordinate origin, then the velocity of light  $c$  at a point with a gravitational potential  $\Phi$  will be given by the relation:  $c = c_0 (1 + \Phi/c^2)$ ”. In Refs. [3, 4], Einstein further emphasized the limited scope of the principle of the constancy of  $c$ : the constancy of  $c$  (and equivalently the Michelson-Morley experimental result and the Lorentz invariance) are valid only *locally*, and thus the variation in  $c$  is not in contradiction with the constancy of  $c$ . Although Einstein eventually did not incorporate his VSL idea into his final 1915-16 GR theory in favor of the Riemannian manifold, his insight of a location-dependent velocity of light is a legitimate pursuit on its own right and merit. While the geometrical approach proved successful in accounting for the Solar System Phenomenology at Einstein’s time, the possibility of VSL could yet provide crucial hints into the challenges that scientists currently encounter beyond the solar system; in particular, the nature of the  $\Omega_\Lambda$  component in the  $\Lambda$ CDM model and that of the acceleration discovered in Type Ia supernovae.

The Friedmann equations are based on GR and extrapolate the theory into the cosmic domain. This extrapolation embodies a major assumption in cosmology, as summarized in the Review [20]. Despite GR’s successes in accounting for the Solar System Phenomenology, *is it safe to extrapolate GR into the cosmic domain without prudently considering Einstein’s 1911 idea regarding VSL [2–4]?* While negligible in the solar system, on the cosmic scale, the impact of variation in  $c$  can accumulate, and as our analysis expounded, may manifest in the accelerating expansion that is observed in Type Ia supernovae.

If the critical expansion mode can be justified theoretically, the ground-breaking ‘1998 discoveries of the acceleration [18, 19] could qualify as evidence in support of a decreasing velocity of light as the universe expands.<sup>7</sup>

<sup>7</sup> In our follow-up report [34], we shall provide the theoretical basis in support of the critical expansion mode,  $a \propto t^{2/3}$ , and the variation rule  $c \propto a^{-1/2}$  for the VSL universe.

## B. Role of local scale of gravitationally-bound regions in the estimate of the Hubble constant

Let us turn to Agent #2. The full consideration presented in Section IV A was based on Formula (56) in conjunction with (57). Given the values of the pair  $(\mu, \epsilon)$ , we found the “optimal” combination of  $\{t_0, F_\infty, \kappa\}$  which minimizes  $\chi^2$ , defined in (61). The result for the “optimal”  $F_\infty$  is shown in Fig. 12 for  $\mu = 1/2, 2/3, 1$  and  $\epsilon$  in the range  $[-0.5, 1]$ . At  $\epsilon = 0$ , the luminosity distance-redshift formula (56) is independent of  $\mu$ . Thus, in Fig. 12, all 3 curves thus cross at  $F_\infty^* \approx 0.9$  and  $\epsilon = 0$  (whereas  $\kappa^* \approx 5.2$  and  $t_0^* \approx 13.9$  Gy).

Although we only invoked a parsimonious function, Eq. (57), to model the variation in the local scale, the result obtained in Figure 12 is intuitive and promising. For a wide range of  $\epsilon$ , the value  $F_\infty$  is smaller than 1, meaning that the high- $z$  emitters corresponded to a smaller local scale. With  $F_\infty^* \approx 0.9$  and  $\kappa^* \approx 5.2$ , Figure 6 depicts a monotonic increase of the local scale as the universe expands. It indicates that the gravitationally-bound regions *cannot* fully resist cosmic expansion. As the global scale expanded, the galaxies also expanded by about 10% larger over the course of time since the recombination event, with the crossover occurring at  $z^* = 1/\kappa^* \approx 0.2$ . High- $z$  gravitationally-bound regions that contained distant supernovae thus had a local scale which is 10% smaller than the local scale of our Solar System at our current time.

An interesting question naturally arises: Considering that the Cosmic Microwave Background (CMB) corresponded to a region of very high  $z$  ( $\sim 1,100$ ), should the CMB analysis take into account the 10-percent reduction in the local scale for high- $z$  regions, as encoded in the value of  $F_\infty^* \approx 0.9$ ?

This is a tantalizing possibility: the 10-percent reduction in the local scale for early-time emitters uncovered in our analysis curiously happens to be of similar magnitude as the discrepancy in the value of  $H_0$  when extracted from the CMB ( $H_0 \approx 67$ ) [24–33] versus the one obtained from late-time objects ( $H_0 \approx 74$ ) [21–23], a 9% difference. It would be interesting to see whether the tension in the estimates of  $H_0$  may be rooted in the variation of the local scale.

In what follows, we would suggest for such a potential connection. With the aid of the age formula (32), we convert Eq. (68) into:

$$\frac{d_L^{[loc]}}{c_{SS}} = \frac{\mu}{F(z)H_0} (1+z) \ln(1+z) \quad (74)$$

The “effective” value of the Hubble constant for a given  $z$  can be read off as  $H_0^{\text{eff}}(z) := F(z)H_0$ . With  $F(z \rightarrow 0) = 1$  and  $F(z \rightarrow \infty) = F_\infty^*$ , the “effective” Hubble constant

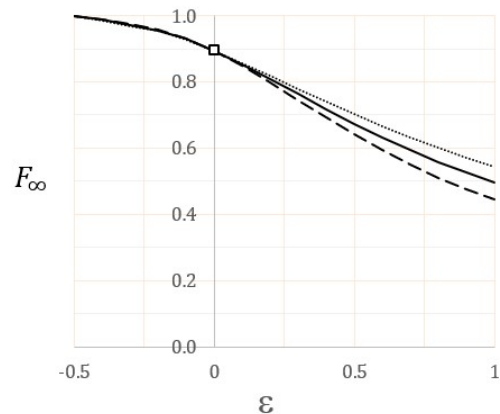


Figure 12:  $F_\infty$  as function of  $\epsilon$ . Solid line:  $\mu = 2/3$ ; dashed line:  $\mu = 1/2$ ; dotted line:  $\mu = 1$ . All 3 lines cross at  $\{\epsilon^*, F_\infty^*\} = \{0, 0.894\}$  shown by the opened square.

is:

$$H_0^{\text{eff}}(z) = \begin{cases} H_0 & \text{for } z \rightarrow 0 \\ F_\infty^* H_0 & \text{for } z \rightarrow \infty \end{cases} \quad (75)$$

in which  $F_\infty^* \approx 0.9$  as obtained from our VSL fit to the Pantheon data.

This probable “explanation” of the Hubble constant tension via the use of  $H_0^{\text{eff}}(z)$  can be further verified in a simple way. Let us split the Pantheon dataset into 4 quartiles of equal size, each containing 262 supernovae with redshift ranging from the lowest to the highest. The 1<sup>st</sup> quartile corresponds to  $z \in (0.01, 0.13)$ ; the 4<sup>th</sup> quartile to  $z \in (0.4235, 2.26)$ . Next, let us fit the 1<sup>st</sup> quartile and the 4<sup>th</sup> quartile *separately* to the following formula:

$$\frac{d_L^{[loc]}}{c_{SS}} = t_0 (1+z) \ln(1+z) \quad (76)$$

This formula is nothing but (74) with  $t_0$  standing in place of the prefactor  $\mu/(F(z)H_0)$ ;  $t_0$  thus acts as an “effective” parameter that is valid for a given quartile of the dataset. The results of the fit are:

- The 1<sup>st</sup> quartile (lowest  $z$ ) yields  $t_0^{[Q1]} = 14.1$  Gy;
- The 4<sup>th</sup> quartile (highest  $z$ ) yields  $t_0^{[Q4]} = 15.4$  Gy.

There is indeed a 9% difference between  $t_0^{[Q1]}$  and  $t_0^{[Q4]}$ , thus lending support to our tentative “explanation” of the Hubble constant tension.

## VI. SUMMARY

We applied a version of VSL to late-time cosmology. In our consideration, the velocity of light varies as a function of the scale factor in the form  $c \propto a^{-\zeta}$ , first put forth by Barrow in [1]. There is one key departure in our approach however. In [1] the scale factor was intended to mean the global cosmic scale factor. In our approach, the scale factor is also applicable to the local scale factor of the gravitationally-bound regions (namely, galaxies) as well. Densely populated regions (such as galaxies) which contain the emitter sources (e.g., a supernova) or the observer (in this case, the dense region is the Milky Way) are gravitationally-bound and are not subject to cosmic expansion. On the one hand, this aspect is crucial in order for the Earth-based observer being able to detect the redshift. On the other hand, this aspect is a great virtue: Since the Milky Way has resisted the cosmic expansion, it has a different scale from the global cosmic scale of the outer space region that directly encloses it. Thanks to the VSL dependence  $c \propto a^{-\zeta}$ , the velocity of light inside the Milky Way must *differ* from that in the outer space region that directly encloses it. For a lightwave from the outer space entering the Milky Way to reach the Earth-based astronomer, the change in the speed of light at this juncture would force the lightwave to undergo a refraction. This refraction effect alters the wavelength that would eventually reach the astronomer's apparatus.

The refraction effect is what was missing in previous works that attempted to apply VSL to the observational data [12–15]. Without including the refraction effect, one would continue to use the classic Lemaître redshift formula  $1 + z = a^{-1}$ . However, by properly taking into account the refraction effect, we find that the standard Lemaître redshift formula needs be replaced by the *modified* Lemaître redshift formula  $1 + z = a^{-(1+\zeta)}$ . The participation of the VSL exponent  $\zeta$  in the modified Lemaître redshift formula is novel; it holds the key to our re-analysis of the Combined Pantheon Sample in the context of VSL. To the best of our knowledge, our current work is the first to bring the refraction effect to the fore.

In our reformulation of the distance-redshift relations, apart from the RW metric (with  $c$  being allowed to vary), we do *not* rely on any underlying theory of gravitation, such as GR or the Friedmann equations. Our analysis is applicable to a universe which satisfies 2 following parsimonious conditions:

- (I) A variation in the velocity of light as a power-law function of the scale factor:  $c \propto a^{-\zeta}$ . This functional form does not have a preferred scale.
- (II) An evolution for the global cosmic scale factor as a power-law function of “cosmic time”:  $a \propto t^\mu$ . This functional form does not have a preferred time

scale. The flat CDM model is a member (when  $\mu = 2/3$ ) of this family.

The flow of exposition in our work was as follows:

1. Modifying Lemaître's redshift formula: We demonstrated how the VSL rule (I),  $c \propto a^{-\zeta}$ , gives rise to the refraction effect. We highlighted the role of the 3 transits between different regions as a lightwave traveling from a distant emitter to reach the Earth-based astronomer. See Sections III A and III B. The cumulative effects of the 3 transits lead to a new formula for the redshift:

$$1 + z = a^{-(1+\zeta)} F^{1+\zeta}(z) \quad (77)$$

in which the function  $F(z)$  captures the variation in the local scale of gravitationally-bound regions as a function of the redshift. See Section III C.

2. Modifying the distance-vs- $z$  formula: Employing the evolution rule (II),  $a \simeq t^\mu$ , we derived a new distance-vs- $z$  relation:

$$\frac{r}{c_0} = \frac{1}{(1+\zeta)H_0} \int_0^z dz' \frac{F^{\epsilon(1+\zeta)}(z')}{(1+z')^{1+\epsilon}} \quad (78)$$

in which  $1 + \epsilon := \frac{1}{\mu(1+\zeta)}$ . See Section III D.

3. Modifying the luminosity distance-vs- $z$  formula, which is the centerpiece of our study:

$$\frac{d_L^{[loc]}}{c_{SS}} = \frac{t_0(1+\epsilon)}{F(z)}(1+z) \int_0^z dz' \frac{F^{\frac{\epsilon}{\mu(1+\epsilon)}}(z')}{(1+z')^{1+\epsilon}} \quad (79)$$

We further specified the variation of the local scale as a monotonic slowly-varying function of  $z$ :

$$F(z) := F_\infty + (1 - F_\infty) \frac{2}{1 + e^{\kappa z}} \quad (80)$$

See Section III E.

4. General analysis of the Pantheon dataset based on our reformulation of redshift formulae: We applied Formulae (79) and (80) to the Combined Pantheon Sample. We reported the  $\chi^2$  error between our VSL model and the Pantheon data for a 3-d grid  $\{\mu, \epsilon, (1+\epsilon)t_0\}$ . The  $\chi^2$  error is found to be insensitive to the value of  $\mu$ . Moreover, the minimum  $\chi^2$  is consistent with  $\epsilon = 0$ . See Section IV A.
5. Special case,  $\epsilon = 0$ : Based on a generic dimensionality argument, we established a link between  $\zeta$  and  $\mu$ :  $\zeta = 1 - 1/\mu$ , hence justifying  $\epsilon = 0$ . The luminosity distance-vs- $z$  relation is significantly simplified to:

$$\frac{d_L^{[loc]}}{c_{SS}} = \frac{t_0}{F(z)}(1+z) \ln(1+z) \quad (81)$$



It achieves an excellent fit to the Pantheon data with the cosmic age parameter  $t_0^* \approx 13.9$  Gy; and  $F_\infty^* \approx 0.9$  and  $\kappa^* \approx 5.2$  for the function  $F(z)$ . The fit is *indistinguishable* from the  $\Lambda$ CDM model; the absolute moment of the normalized error term  $L_k := \left\langle |(\mu^{\text{Pantheon}} - \mu^{\text{model}})/\sigma|^k \right\rangle^{1/k}$  is almost identical in both models (VSL and  $\Lambda$ CDM) for all orders  $k$  up to 20. See Section IV B.

The parameters in Formulae (80) and (81) are intuitive and have direct physical meanings. In particular:

- The cosmic age  $t_0^* \approx 13.9$  Gy is obtained, without invoking the  $\Lambda$  component.
- The value of  $F_\infty^* \approx 0.9$  indicates a 10% reduction in the “effective” value of  $H_0$  if the latter is estimated from high- $z$  portion of the Pantheon dataset, as compared with the value of  $H_0$  estimated from low- $z$  portion of the Pantheon dataset.

Two important implications emerge from our analysis:

- [A] We offer a viable interpretation of the accelerating expansion on the sole basis of variable speed of light, in place of the  $\Lambda$  component. See Section V A.
- [B] As a by-product, the role of  $F(z)$  might shed a refreshing perspective onto the ongoing tension in the estimate of the Hubble constant using the CMB versus that derived from late-time objects [21–33]. See Section V B.

In conclusion, the Pantheon SNeIa dataset is consistent with a variable-light-speed scenario in which  $a \propto t^\mu$  and  $c \propto a^{1-1/\mu}$  with  $\mu$  left *unspecified*. In a universe which expands as  $a \propto t^{2/3}$ , the velocity of light would vary as  $c \propto a^{-1/2}$ .

A theoretical basis for the VSL form  $a \propto t^{2/3}$  and  $c \propto a^{-1/2}$  will be provided in our follow-up report, Ref. [34].

### Acknowledgments

The idea of applying VSL in Barrow’s form,  $c \propto a^{-\zeta}$ , to the Pantheon dataset sprang out of the author’s communications with Viktor Toth, who also generously offered us insightful theoretical guidance during the development of our work. The author thanks Richard Shurtleff and Vesselin Gueorguiev for their constructive feedbacks; and Richard Shurtleff, Juha Korpela, and Lucas Lombriser for their meaningful encouragements.

Our numerical tool (1Mb) and the output of our analysis presented in Section IV are available upon request.

### Appendix A: An equivalent derivation of the modified Lemaître redshift formula

We produce an alternative route by way of frequency transformation to modifying Lemaître’s redshift formula (26). The modified RW metric (5) can be recast as:

$$ds^2 = a^2(t) \left[ \frac{c_0^2}{a^{2+2\zeta}(t)} dt^2 - \frac{dr^2}{1 - kr^2} - r^2 d\Omega^2 \right] \quad (\text{A1})$$

The null geodesic ( $ds^2 = 0$ ) for a lightwave traveling from an emitter toward Earth (viz.  $d\Omega = 0$ ) is thus:

$$\frac{c_0 dt}{a^{1+\zeta}(t)} = \frac{dr}{\sqrt{1 - kr^2}} \quad (\text{A2})$$

Denote  $t_e$  and  $t_o$  the emission and observation time points of the lightwave, and  $r_e$  the co-moving distance of the galaxy from Earth. From (A2), we have:

$$\int_{t_e}^{t_o} \frac{c_0 dt}{a^{1+\zeta}(t)} = \int_{r_e}^0 \frac{dr}{\sqrt{1 - kr^2}} \quad (\text{A3})$$

The next wavecrest to leave the emitter at  $t_e + \delta t_e$  and arrive at Earth at  $t_o + \delta t_o$  satisfies:

$$\int_{t_e + \delta t_e}^{t_o + \delta t_o} \frac{c_0 dt}{a^{1+\zeta}(t)} = \int_{r_e}^0 \frac{dr}{\sqrt{1 - kr^2}} \quad (\text{A4})$$

Subtracting the two equations yields:

$$\frac{\delta t_o}{a^{1+\zeta}(t_o)} = \frac{\delta t_e}{a^{1+\zeta}(t_e)} \quad (\text{A5})$$

which leads to the ratio between the emitted frequency and the observed frequency:<sup>8</sup>

$$\frac{\nu_o}{\nu_e} = \frac{\delta t_e}{\delta t_o} = \frac{a^{1+\zeta}(t_e)}{a^{1+\zeta}(t_o)} = \frac{a_e^{1+\zeta}}{a_o^{1+\zeta}} \quad (\text{A7})$$

<sup>8</sup> In previous VSL analyses [12–14], it was correctly reported, due to Eq. (A7), that

$$\frac{\lambda_o}{\lambda_e} = \frac{c_o/\nu_o}{c_e/\nu_e} = \frac{c_o}{c_e} \frac{\nu_e}{\nu_o} = \frac{a_o^{-\zeta}}{a_e^{-\zeta}} \cdot \frac{a_o^{1+\zeta}}{a_e^{1+\zeta}} = \frac{a_o}{a_e} \quad (\text{A6})$$

which is identical to the classic consideration of non-variable speed of light. However, that fact alone is not sufficient to conclude that the classic Lemaître redshift formula remains valid for VSL. The reason is that  $\lambda_o$  is *not* what the Earth-based astronomer observes. To reach the astronomer, the lightwave needs to enter the *gravitationally-bound* Milky Way which has a scale *smaller* than the current global cosmic scale. Per  $c \propto a^{-\zeta}$ , the velocity of light  $c_o^{[loc]}$  inside the Milky Way is different from the velocity of light  $c_o$  in the outer space region that encloses the Milky Way. The lightwave thus gets refracted during its entry to the Milky Way, with its wavelength getting altered to  $\lambda_o^{[loc]} = \lambda_o c_o^{[loc]}/c_o$  per Eq. (17). It is the wavelength  $\lambda_o^{[loc]}$  which gets registered in the astronomer’s apparatus.

For transits between local regions to global regions (i.e., Transit #1 and Transit #3 in Fig. 1 in Page 4), since  $\lambda \propto c$ , the frequency is:

$$\nu = \frac{c}{\lambda} = \text{const} \quad (\text{A8})$$

This means that the frequency of the lightwave does not change during Transit #1 and Transit #3, viz.

$$\nu_e^{[loc]} = \nu_e \quad (\text{A9})$$

$$\nu_o^{[loc]} = \nu_o \quad (\text{A10})$$

Given that

$$\lambda_o^{[loc]} = \frac{c_o^{[loc]}}{\nu_o^{[loc]}} \quad (\text{A11})$$

$$\lambda_e^{[loc]} = \frac{c_e^{[loc]}}{\nu_e^{[loc]}} \quad (\text{A12})$$

$$\frac{\lambda_o^*}{\lambda_e^{[loc]}} = \frac{a_o^{[loc]}}{a_e^{[loc]}} \quad (\text{A13})$$

we have:

$$\frac{\lambda_o^{[loc]}}{\lambda_o^*} = \frac{\lambda_o^{[loc]}}{\lambda_e^{[loc]}} \cdot \frac{\lambda_e^{[loc]}}{\lambda_o^*} \quad (\text{A15})$$

$$= \frac{c_o^{[loc]}}{c_e^{[loc]}} \cdot \frac{\nu_e}{\nu_o} \cdot \frac{a_e^{[loc]}}{a_o^{[loc]}} \quad (\text{A16})$$

$$= \left( \frac{a_o^{[loc]}}{a_e^{[loc]}} \right)^{-\zeta} \cdot \frac{a_o^{1+\zeta}}{a_e^{1+\zeta}} \cdot \frac{a_e^{[loc]}}{a_o^{[loc]}} \quad (\text{A17})$$

Finally:

$$1 + z := \frac{\lambda_o^{[loc]}}{\lambda_o^*} = \left( \frac{a_e}{a_o} \right)^{-(1+\zeta)} \left( \frac{a_e^{[loc]}}{a_o^{[loc]}} \right)^{1+\zeta} \quad (\text{A18})$$

in perfect agreement with (26).

- 
- [1] J.D. Barrow, Phys. Rev. D 59, 043515 (1999); arXiv:astro-ph/9811022
- [2] A. Einstein, Annalen der Physik 35, 898-908 (1911)
- [3] A. Einstein, Annalen der Physik 38, 355-369 (1912)
- [4] A. Einstein, Annalen der Physik 38, 1059-1064 (1912)
- [5] J. W. Moffat, Int. J. Mod. Phys. D 2, 351 (1993); arXiv:gr-qc/9211020
- [6] A. Albrecht and J. Magueijo, Phys. Rev. D 59, 043516 (1999); arXiv:astro-ph/9811018
- [7] J.D. Barrow and J. Magueijo, Phys. Lett. B 443, 104 (1998); arXiv:astro-ph/9811072
- [8] J.D. Barrow and J. Magueijo, Astrophys. J., 532:L87-L90 (2000); arXiv:astro-ph/9907354
- [9] J. Magueijo and L. Smolin, Phys. Rev. Lett. 88, 190403 (2002); arXiv:hep-th/0112090
- [10] J. Magueijo, Rept. Prog. Phys. 66, 2025 (2003); arXiv:astro-ph/0305457
- [11] J. Magueijo and J. W. Moffat, Gen. Rel. Grav. 40, 1797-1806 (2008); arXiv:0705.4507
- [12] P. Zhang and X. Meng, Mod. Phys. Lett. A Vol. 29, No. 24, 1450103 (2014); arXiv:1404.7693 [astro-ph.CO]
- [13] J-Z. Qi, M-J. Zhang, and W-B. Liu, Phys. Rev. D 90, 063526 (2014); arXiv:1407.1265 [gr-qc]
- [14] A. Ravanpak, H. Farajollahi, and G.F. Fadakar, Res. Astron. Astrophys., 17 (2017) 26; arXiv:1703.09811
- [15] V. Salzano and M.P. Dąbrowski, Astrophys. J. 851, 97 (2017); arXiv:1612.06367
- [16] D.M. Scolnic; Jones, D.O.; Rest, A.; Pan, Y.C.; Chornock, R.; Foley, R. J.; Huber, M. E.; Kessler, R.; Narayan, G.; Riess, A. G.; et al. , Astrophys. J. 859 (2), 101 (2018)
- [17] The Pantheon dataset is downloadable from: <https://archive.stsci.edu/hlsp/ps1cosmo/scolnic/>
- [18] A. Riess et al, Astron. J. 116, 1009 (1998)
- [19] S. Perlmutter et al, Astron. J. 517, 565 (1999)
- [20] P. Bull, Y. Arkrami, et al, “Beyond  $\Lambda$ CDM: Problems, solutions, and the road ahead”, Physics of the Dark Universe 12 (2016) 56; arXiv:1512.05356. See Section 3.1 by P.G. Ferreira for discussions
- [21] A. G. Riess, S. Casertano, W. Yuan, L. M. Macri, and D. Scolnic, Astrophys. J. 876, 85 (2019), arXiv:1903.07603 [astro-ph.CO]
- [22] M. J. Reid, D. W. Pesce, and A. G. Riess, Astrophys. J. 886, L27 (2019), arXiv:1908.05625 [astro-ph.GA]
- [23] K. C. Wong et al., (2019), arXiv:1907.04869 [astro-ph.CO]
- [24] N. Aghanim et al. (Planck), (2018), arXiv:1807.06209 [astro-ph.CO]
- [25] T. M. C. Abbott et al. (DES), Mon. Not. Roy. Astron. Soc. 480, 3879 (2018), arXiv:1711.00403 [astro-ph.CO]
- [26] O. H. Philcox, M. M. Ivanov, M. Simonović, and M. Zaldarriaga, (2020), arXiv:2002.04035 [astro-ph.CO]
- [27] A. Cuceu, J. Farr, P. Lemos, and A. Font-Ribera, (2019), arXiv:1906.11628 [astro-ph.CO]
- [28] N. Schöneberg, J. Lesgourgues, and D. C. Hooper, (2019), arXiv:1907.11594 [astro-ph.CO]
- [29] M. M. Ivanov, M. Simonović, and M. Zaldarriaga, (2019), arXiv:1909.05277 [astro-ph.CO]
- [30] G. D’Amico, J. Gleyzes, N. Kokron, D. Markovic, L. Senatore, P. Zhang, F. Beutler, and H. Gil-Marín, (2019), arXiv:1909.05271 [astro-ph.CO]
- [31] T. Colas, G. D’Amico, L. Senatore, P. Zhang, and F. Beutler, (2019), arXiv:1909.07951
- [32] P. Lemos, E. Lee, G. Efstathiou, and S. Gratton, Mon. Not. Roy. Astron. Soc. 483, 4803 (2019), arXiv:1806.06781 [astro-ph.CO]
- [33] E. Aubourg et al., Phys. Rev. D92, 123516 (2015), arXiv:1411.1074 [astro-ph.CO]
- [34] H. Nguyen, *A theoretical basis of variable velocity of light for late-time cosmology* (in preparation)